Geoderma 426 (2022) 116095

Contents lists available at ScienceDirect

Geoderma

journal homepage: www.elsevier.com/locate/geoderma

Soil spectroscopy with the Gaussian pyramid scale space

Thorsten Behrens [a,b,*], Raphael A. Viscarra Rossel [c], Leonardo Ramirez-Lopez [d], Philipp Baumann [a]

[a] Swiss Competence Center for Soil, School of Agricultural, Forest and Food Sciences, Bern University of Applied Sciences, Länggasse 85, CH-3052, Zollikofen, Switzerland
[b] Soil and Spatial Data Science, Soilution GbR, Heiligegeiststrasse 13, 06484 Quedlinburg, Germany
[c] Soil and Landscape Science, School of Molecular and Life Sciences, Faculty of Science and Engineering, Curtin University, GPO Box U1987, Perth, WA 6845, Australia
[d] Data Science department, BUCHI Labortechnik AG, Meierseggstrasse 40, 9230 Flawil, Switzerland

ARTICLE INFO

Handling Editor: Budiman Minasny

Keywords:
Gaussian pyramid scale space
Soil spectroscopy
Feature engineering
Feature importance
Interpretable machine learning

ABSTRACT

Soil visible-near infrared (vis–NIR) spectra are complex and modeling soil properties can be challenging. They can suffer from additive and multiplicative noise, they are hyper-dimensional and highly collinear, making their analyses and interpretation sometimes difficult. Here, we introduce the Gaussian pyramid scale space as a multi-resolution approach for denoising spectra, reducing dimensionality, and improving the interpretability and accuracy of spectroscopic machine learning. We also used the approach to analyse contextual interactions between different resolutions and the stability of feature importance across different resolutions. Using an Australian data set and the German data in the LUCAS spectral database we found that with a single Gaussian scale that represents a relatively coarse spectral resolution, we could estimate organic carbon, clay and pH as accurately as with multiple Gaussian scales, or using all resolutions. This indicates that, in the vis–NIR range, there are no relevant interactions between resolutions, which simplifies interpretations. We conclude that the Gaussian pyramid scale space can help to model soil properties with spectral machine learning, improving both accuracy and interpretability. Because the Gaussian pyramid approach is computationally efficient, it can also be used for preprocessing and knowledge discovery before more elaborate modeling is applied.

1. Introduction

Soil visible-near infrared (vis–NIR) spectra are complex and difficult to model. They can suffer from additive and multiplicative noise (Stenberg et al., 2010) and they are hyper-dimensional and highly collinear, making their analyses and interpretation challenging.

The information that the soil vis–NIR spectra contain is in the shape and intensity of their diffuse reflectance (or inversely, their absorptions) that represent the interactions of the soil material with electromagnetic radiation. The data consist of reflectance values in adjacent narrow wavelength intervals. To extract the relevant information from the data is not trivial, not at least because the data is strongly correlated. Commonly, techniques for dimensionality reduction such as partial least squares (PLS, Wold et al., 2001) are used for modeling and prediction. The challenge for the analysis of vis–NIR reflectance spectra is therefore how to extract useful information from the spectra, which consists of localised physicochemical features, and 'noisy' and strongly correlated data.

Here, we present an approach based on the Gaussian pyramid scale space (Burt and Adelson, 1983; Behrens et al., 2018a; Behrens et al., 2018b) for preprocessing soil spectra. The Gaussian pyramid is a hierarchical dyadic sequence of spectral covariate datasets, where a coarser scale or resolution, also called octave, is generated by reducing the wavelength count by one half (Burt and Adelson, 1983), following a Gaussian filtering step.

This approach is related to wavelet analysis (Bruce and Li, 2001; Shao and Ma, 2003; Jacques et al., 2011; Lindeberg, 2015), which have been used in several studies on soil spectroscopy, e.g. Viscarra Rossel et al. (2016), Ge et al. (2007), Viscarra Rossel and Behrens (2010) and Song et al. (2021). Specifically, they share the property that they denoise and decompose a signal at specific scales or resolutions, which can improve the quantitative analysis of spectra for prediction (Viscarra Rossel and Lark, 2009). The Gaussian pyramid, or more precisely the related Laplacian pyramid, which is build from differences between

* Corresponding author at: Swiss Competence Center for Soil, School of Agricultural, Forest and Food Sciences, Bern University of Applied Sciences, Länggasse 85, CH-3052, Zollikofen, Switzerland.
E-mail address: thorsten.behrens@bfh.ch (T. Behrens).

https://doi.org/10.1016/j.geoderma.2022.116095
Received 27 May 2022; Received in revised form 4 August 2022; Accepted 7 August 2022
Available online 13 August 2022

consecutive Gaussian octaves and forms a pyramid of high pass filters or estimates of second order derivatives, is closely related to the Mexican hat wavelet, which also has been applied for soil spectroscopy (Vohland et al., 2016). Wavelets are complete representations (linear independent or orthogonal basis functions) which are mostly used for denoising and data compression. In contrast, the Gaussian scale space is an over-complete (not linearly independent) representation (Smith, 2018; Guerrero-Colon et al., 2008). This redundancy is of advantage over non-redundant representations when robustness is required, as in image matching or digital soil mapping, and where additional intermediate scales further help to increase robustness and thus precision or prediction accuracy (Smith, 2018; Guerrero-Colon et al., 2008; Lowe, 1999; Lindeberg, 2015; Behrens et al., 2018a).

We use the Gaussian pyramid to be able to easily apply and test different derivatives (first and second order) on the Gaussian scales. Most publications published so far dealing with the use of wavelets in soil spectroscopy, focused on the modeling with the wavelet coefficients, which, in the case of commonly used Daubechies and Mexican hat wavelets (Viscarra Rossel and Lark, 2009; Vohland et al., 2016), correspond to the second order derivative only.

Our aims here are to explore the use of the Gaussian pyramid with vis–NIR spectra to: (i) denoise and systematically resample spectra in order to improve the predictive and explanatory accuracy of spectroscopic machine learning on single and combined scales and with different derivatives, and (ii) explore the presence of contextual cross-resolution interactions in the spectra. Our hypothesis is that such contextual cross-resolution interactions occur due to differences in sensor characteristics (cf. Section 2.6.1 and Section 2.6.2) and the physics of energy absorption by the soil constituents, which vary across the spectrum (Ge et al., 2007; Viscarra Rossel and Behrens, 2010). Hence, a potentially optimal resolution is expected to also vary across the spectrum, e.g. the resolution required at 700 nm might be different to the resolution required at 2100 nm, because generally the longer the wavelength the narrower the absorption features.

The experiments were performed with vis–NIR spectra from an Australian dataset and the part of the LUCAS database available for Germany. We built models for soil organic carbon (OC) and clay content for the Australian data set and additionally for the pH-value for the LUCAS data set.

2. Methods

2.1. The Gaussian pyramid scale space

A Gaussian pyramid is a hierarchical, multi-resolution (or multi-scale) representation of a signal, originally developed for multi-scale image analysis (Burt and Adelson, 1983; Adelson et al., 1983) and is used in many disciplines from image processing and computer vision to digital soil mapping (Burt and Adelson, 1983; Lowe, 1999; Behrens et al., 2018a; Behrens et al., 2018b).

The scale decomposition in the Gaussian pyramid is based on two operations, smoothing and scaling, which are used to successively to reduce the resolution by half. A spectral pyramid is therefore a dyadic sequence $S_i, S_{i-1}, \ldots, S_0$ of spectra (Fig. 2). S_i has the same dimension and resolution as the original spectra and S_{i-1} is derived from S_i by reducing the number of spectral wavelenghts by half. S_0 is the theoretically coarsest resolution consisting of one reflectance value only (Sonka et al., 2014).

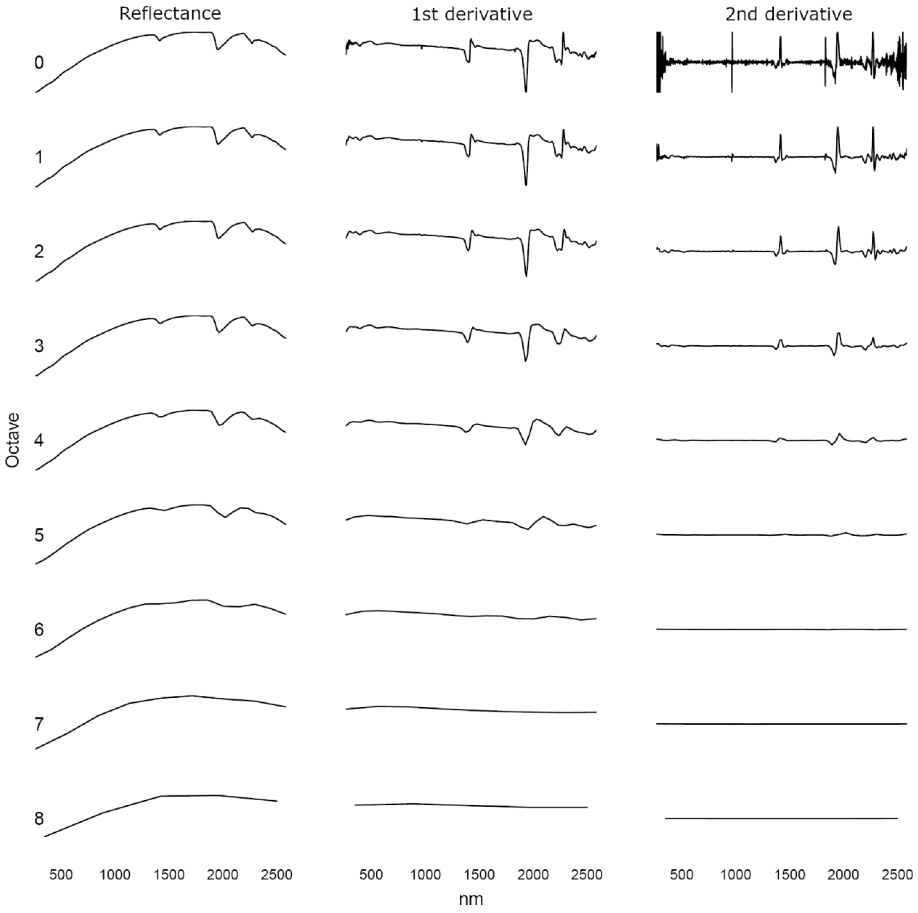

Fig. 2. Reflectance, 1st derivative and 2nd derivative for the first 8 octaves (including the original reflectance data, octave 0) of the Gaussian pyramid, based on the average spectra of the Australian dataset.

Each downscaling step is computed by convolving the spectra with a Gaussian blur filter (Getreuer, 2013) followed by the actual downscaling step where all even-numbered wavelengths are removed. The Gaussian blur filter is used to avoid aliasing effects that may otherwise occur during downsampling. In this way all resolutions or octaves of the pyramid are constructed (Fig. 1). A mathematical description can be found in Adelson et al. (1983).

In this study we derived 8 octaves from the original spectra, using a 1D Gaussian kernel (Fig. 2). Octave 0 denotes the original spectrum.

2.2. Preprocessing and derivatives

To analyse the sole effect of scaling with the Gaussian pyramid, we do not apply any additional preprocessing such as smoothing, normalization or binning methods (Savitzky and Golay, 1964; Barnes et al., 1989; Gautam et al., 2015). We test the reflectance data as well as the 1st and 2nd order derivatives (D1 and D2) derived from each octave, which are used to reduce additive (baseline) and multiplicative (shape) scattering effects between spectra and in turn can increase generalization accuracy (Blanco et al., 1997; Delwiche and Reeves, 2004; Rinnan et al., 2009; Igne et al., 2010). We use finite differences to compute the 1st and 2nd order derivatives. Fig. 2 shows the reflectance values (D0) for each octave of the Gaussian pyramid and the resulting derivatives D1 and D2.

2.3. Machine learning with Cubist

Cubist is a form of piece-wise linear decision tree (Quinlan, 1993; Kuhn and Quinlan, 2020). It recursively partitions the response variable into subsets defined by 'if' and 'else' rules, which are hierarchically arranged and can be based on a single or on multiple wavelenghts. If a condition is true, an ordinary least-squares regression is fitted using the data within that partition. Otherwise, the rule defines the next node in the tree. The predictions in the terminal node are also based on linear models. The *n* most similar training samples or neighbors are used to build an averaged ensemble prediction for each sample of the rule-based model in cubist. Additionally, comparable to boosting, multiple rule-based models can be combined, which is called committees (Kuhn and Quinlan, 2020).

2.4. Resolution and contextual analysis

To test effects of a joint influence and interactions between wavelengths from different octaves on prediction accuracy, we compared single resolution and two cross-resolution modeling approaches.

2.4.1. Single resolution models

For the single resolution models we extracted each octave of each feature set (reflectance, D1 and D2) to build separate machine learning models. In doing so, we can analyse the changes in validation accuracy

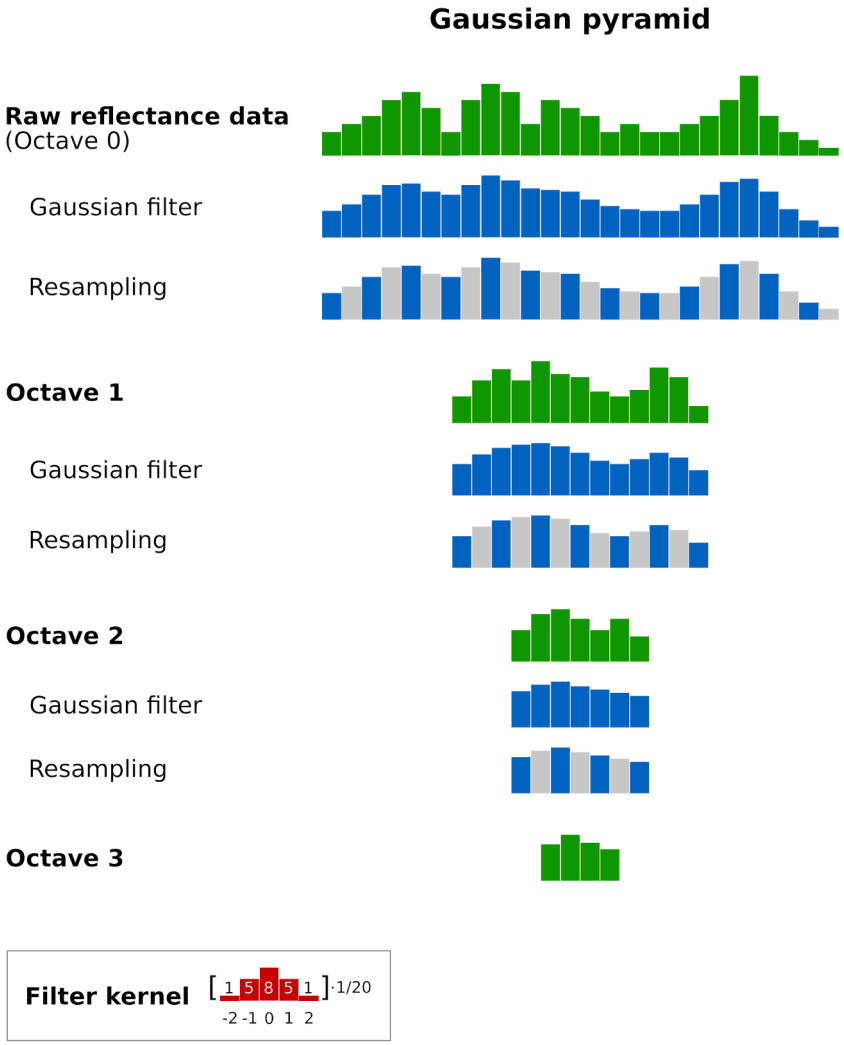

Fig. 1. Filtering and resampling across 4 octaves of a Gaussian pyramid and the corresponding filter kernel used in this study.

across the octaves and for all derivatives. Hence, we can determine which feature set provides the highest predictive accuracy at which resolution.

2.4.2. Full set models

To analyse the joint effect of all octaves, we merged all features of all Gaussian pyramid octaves into a single model by concatenating the spectra of all octaves for each sample. Theoretically, this should provide the overall best results, because all possible features are included and all possible contextual interactions should be covered. However, effects of collinearity and potentially noisy features from fine resolutions as well as confounding effects, might have a negative impact on predictive accuracy. Since this also depends on the machine learning approach, we do not further try to unravel these potential effects in this study.

2.4.3. Additive coarse to fine resolution models

To test the joint effect of multiple octave datasets on predictive accuracy we successively added finer octaves to the model starting with the coarsest octave. This approach should attenuate the negative influences of additive and multiplicative noise, hyper-dimensionality and high collinearity, which are particularly prevalent at finer resolutions. This therefore should allow to detect possible cross-resolution interactions within the relevant range of resolutions, which are found in other disciplines such as spatial data science (Behrens et al., 2018a; Behrens et al., 2019). Thus the resulting models are expected to be at least as good as the full set models. As with the single resolution models, the final additive model, i.e. the best combination of octaves, is selected based on the maximum accuracy achieved after evaluating all combinations.

2.5. Validation and grid learning

To assess the accuracy of the Cubist machine learning models we applied 10-times 10-fold cross-validation for the Australian dataset and 3-times 10-fold cross-validation for the larger LUCAS dataset. We report the R^2 and root mean squared error (RMSE) of the validations.

For tuning the Cubist models we used a grid learning method and tested 0, 1, 3, 5, 7, and 9 neighbors as well as 1, 10, 25, 50, 75, and 100 committees.

2.5.1. Feature importance analysis

We analysed feature importance to visualize and test the stability of the important features across the resolutions in the single resolution modeling approach. Here, we used the relative cubist variable-usage statistics (Kuhn and Quinlan, 2020). The primary aim is to analyse the changes in feature importance across the octaves, because such changes would result in different interpretations. If the assumption that a high predictive accuracy is required for a high explanatory accuracy (Murdoch et al., 2019) holds true, the single Gaussian pyramid octave with the highest validation accuracy should provide the basis for the most reliable interpretations.

2.6. Data sets

2.6.1. Australia

The soil samples of the Australian dataset originated from Queensland, New South Wales, South Australia and Western Australia and were not sampled specifically for this work (Viscarra Rossel and Lark, 2009). Soils were sampled from different layers. Laboratory analysis of air-dried and ground ($\leqslant 2mm$) samples were performed according to the methods described in Viscarra Rossel and Behrens (2010).

The diffuse reflectance spectra of 742 soil samples were measured using the Agrispec vis–NIR spectrometer (Analytical Spectral Devices, Boulder, Colorado,USA) with a spectral range of 350–2500 nm. The spectral resolution of the dataset was 2 nm. Internally the spectrometer has a resolution of 3 nm at 700 nm and 10 nm at 1400 nm/2100 nm, but provides data at 1.4 to 2 nm.

2.6.2. LUCAS, Germany

The LUCAS 2015 topsoil dataset is a European vis–NIR library of topsoil samples (Stevens et al., 2013; Tóth et al., 2013; Jones et al., 2020). We selected all samples located in Germany (LUCAS-DE) and removed all samples which did not comprise a full set of soil property analysis. This resulted in 1793 observations.

The spectra with a range of 400–2500 nm and with a spectral resolution of 0.5 nm were measured using a FOSS XDS Rapid Content Analyzer (FOSS NIR Systems Inc., Laurel, MD, USA). Same as the Agrispec the XDS Rapid Content Analyzer is a multi detector system. Due to artifacts in these spectra we removed the range between 400 to 480 nm, as suggested in Stevens et al. (2013). Finally, we resampled the data provided at a resolution of 0.5 nm to a resolution of 1 nm and used reflectance data for modeling.

3. Results and discussion

3.1. The Gaussian pyramid scale space

3.1.1. Single octave models

The results of the single octave cubist models show that on average as well as for the maximum validation accuracies the medium-scale octaves return the highest validation accuracies (Fig. 3 and 4). Overall the best models are based on octave 3, which, based on the initial resolutions of 1 nm and 2 nm, equals a resolution of 8 nm and 16 nm, respectively. Octaves 6 and 7 with resolutions $>$ 64 nm and 128 nm are too coarse for reasonable modeling, whereas modeling with the original resolutions is affected either by noise or and/or by collinearity. These results reflect the fact that, in the vis–NIR region, the spectral features of the light absorbing components of the soil are usually wider ($\gtrapprox$ 8 nm; (McCarty et al., 2002; Viscarra Rossel et al., 2006)).

In most cases D1 returned the most accurate validations (Table 1). Even though, the differences between D1 and D2 are generally small, we suggest to test both to determine the optimal derivative when working with the Gaussian pyramid. The raw reflectance data is less resolution dependent compared to the derivatives and in most cases it showed, on average, the smallest increase in accuracy across the first four octaves. Figs. 3 and 4 show that the higher the order of the derivative the coarser the best average resolution. This is related to noise in the reflectance data which is emphasized in the derivatives and proportionally amplified with the order of the derivative. The final differences in terms of R^2 between the best single octave raw data model and the best single octave derivative model is up to 6 percent for clay content of the LUCAS-DE dataset.

3.1.2. Cross-resolution models

To analyse the effect of noisy and highly collinear predictors as well as to test if there is additional relevant information in the context, i.e. in a mixture of octaves, we built models of all features across all resolutions and used the additive coarse to fine resolution modeling approach.

Interestingly, the single octave modeling approaches outperform modeling with the full features set. It is also on par with the additive approach with minimal differences in both datasets. There is a slight advantage for the additive approach for the LUCAS-DE data and a similar advantage for the single resolution approach for the Australian data.

The inclusion of finer resolution octaves in the additive approach generally increases the prediction accuracy up to a certain resolution. From there on, the prediction accuracy decreases as additional octaves of finer resolution are added to the model. The finest octave that gives the best prediction accuracy in the additive approach is similar to the octave of the best single resolution model. This shows that there is no substantial information gain or contextual relationships when using multiple resolutions in a single model. This also shows the robustness of

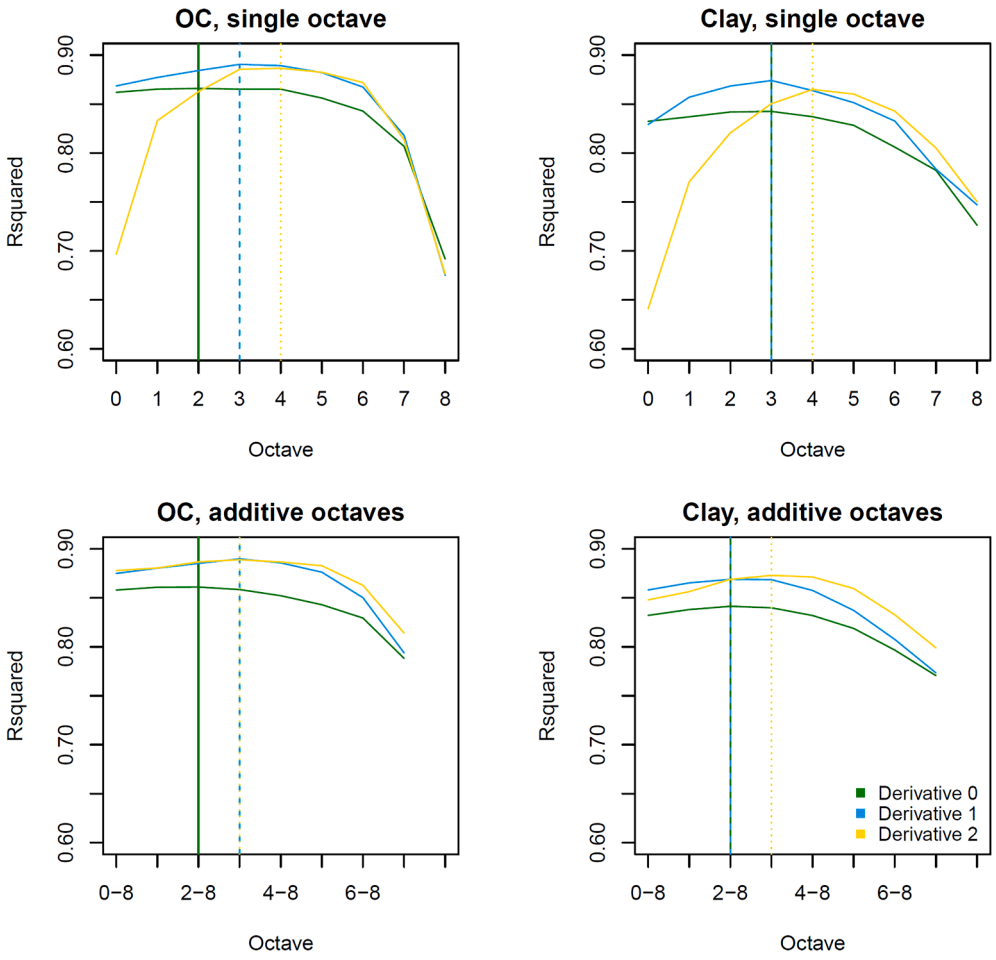

Fig. 3. Predictive accuracy $[R^2]$ of the different single or combined (additive) resolution models for clay and organic carbon (OC) of the Australian dataset based on cubist. The vertical lines mark the octaves or additive octaves of the respective highest model accuracies.

the approach against noise as well as the stability of the single octave approach (cf. Section 3.1.1).

3.1.3. *Feature importance across Gaussian octaves*

An advantage of the single resolution approach is that feature importance can be analysed separately for each octave, which can be important for interpreting the modeling results. Based on the results presented in this study interpretation should be conducted for the resolution with the highest validation accuracy.

Figs. 5 and 6 show the feature importance of D1 and D2 for the first six octaves for clay content for the Australian dataset as an example. It shows a pronounced change in the importance of spectral regions from octave 0 to octave 3, especially for D2. While at the original resolution the regions between 600–800 nm, 1400 nm and 1900 nm are most important for D1 and D2, the region around 2150 nm is important as well regarding D1. At octave 1 the importance of the 600–800 nm range is reduced for both derivatives. The important regions at octave 3, which is the octave with the highest predictive accuracy, are much more consistent between the derivatives and show 6 important regions located approximately between 450–650 nm, 1300–1500 nm, 1600–1900 nm, 1900–2000 nm and 2100–2200, and 2300–2400 nm. These regions are representative of iron oxides (hematite and goethite) but also organic matter, Al–OH in clay minerals, organic matter, as well as water present in interlayers of 2:1 clay minerals such as smectite, kaolinite and illite, respectively, and were also identified in other studies (Viscarra Rossel and Behrens, 2010). The changes in importance across the octaves, especially for D2, clearly shifts the interpretation towards clay minerals. Similar effects are visible for OC content as well (data not shown). The relative increase in significance at 2200–2400 nm is likely due to a decrease in noise from octave 3 onward.

Looking at the same property for the LUCAS-DE dataset shows comparable effects (Fig. 7 and 8). The range between 500 nm and 1300 nm seems to be irrelevant for interpreting clay content on the original resolution of D1. At octave 3 this has changed.

Moreover, there are significant differences between the 1st and 2nd derivatives in the two data sets when interpreting the relationship between the spectra and clay content based on octave 0. However, on octave 3 the interpretations would be rather similar even across the different datasets representative for temperate and tropical soil chemistry.

4. Related methods

One of the most interesting features of the Gaussian pyramid scale space is its technical simplicity and robustness. This could be an advantage over other approaches like the closely related wavelet transforms or convolutional neural networks (CNN).

Viscarra Rossel and Lark (2009) presented an approach based on wavelet coefficients that orders the data of multiple resolutions along their variances and used this as a basis to create parsimonious cross-resolution models. The multi-resolution approaches presented here can also be applied to wavelets and the variance ordering approach to Gaussian pyramid data. Consequently, future research should compare these two concepts for soil spectroscopy. The same holds true for other data reduction approaches such as the uniform-interval wavelength reduction (Yang et al., 2012).

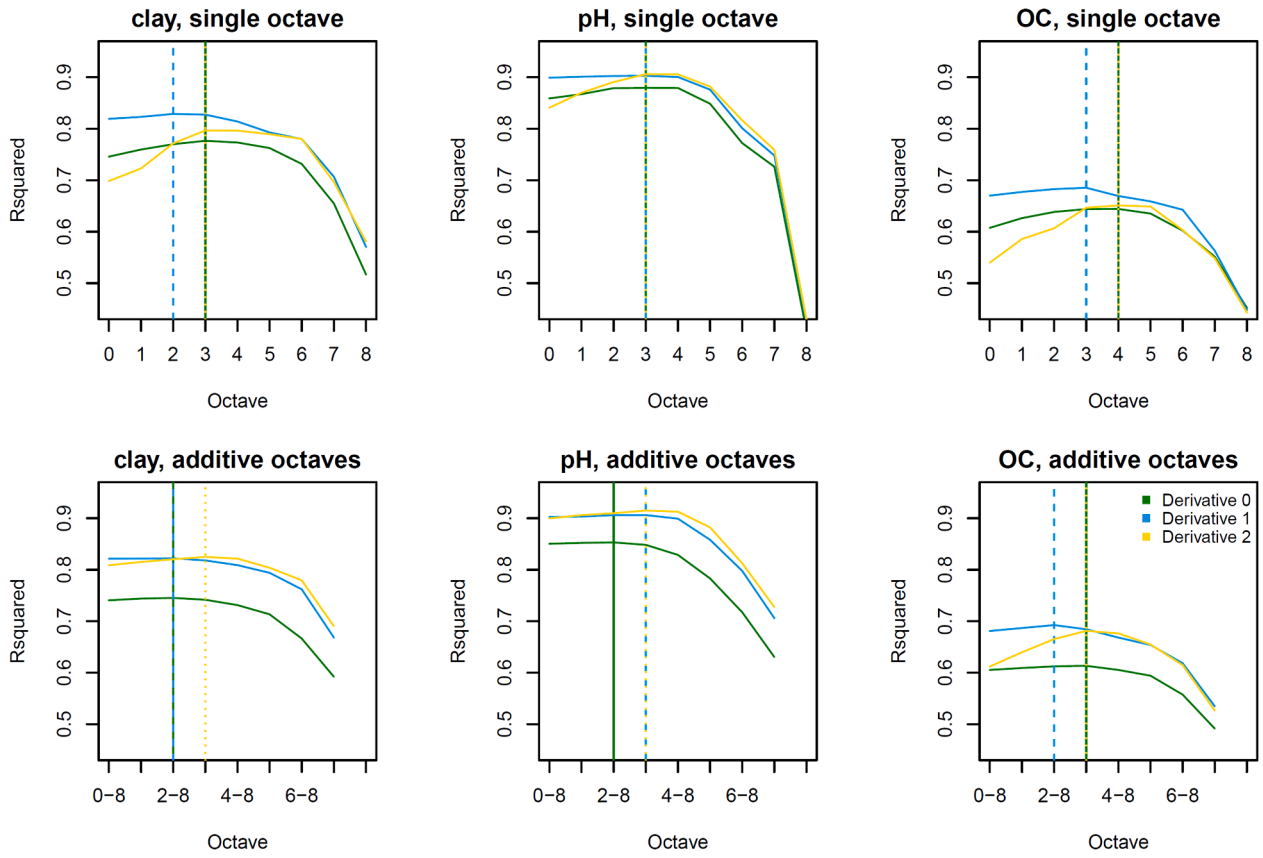

Fig. 4. Predictive accuracy [R^2] of the different single or combined (additive) resolution models for clay and organic carbon (OC) of the LUCAS-DE dataset based on cubist. The vertical lines mark the octaves or additive octaves of the respective highest model accuracies.

Table 1
Cross-validated vis–NIR modeling results for best single resolution (single), full set and additive coarse to fine resolution (additive) cubist models with Gaussian pyramid inputs. AUS is the Australian dataset (Viscarra Rossel and Lark, 2009). LUCAS-DE is the subset of the LUCAS collection from Germany. OC is the organic carbon content.

Data	Property	Method	Deriv.	Octave	Features	RMSE	R^2
AUS	OC [%]	Single	1	3	135	0.74	0.89
		Full set	2	0–8	2151	0.79	0.88
		Additive	1	3–8	268	0.75	0.89
	Clay [%]	Single	1	3	135	6.60	0.87
		Full set	1	0–8	2151	7.00	0.86
		Additive	2	3–8	268	6.62	0.87
LUCAS-DE	OC [g/kg]	Single	1	2	504	14.10	0.69
		Full set	1	0–8	4021	14.19	0.68
		Additive	1	2–8	1001	14.09	0.69
	Clay [%]	Single	1	2	504	4.88	0.83
		Full set	1	0–8	4021	4.99	0.82
		Additive	2	2–8	1001	4.94	0.83
	pH	Single	2	3	252	0.38	0.91
		Full set	1	0–8	4021	0.37	0.90
		Additive	2	3–8	497	0.36	0.92

One of the latest additions to the soil spectroscopy toolbox is CNNs (Liu et al., 2018; Padarian et al., 2019; Shen and Viscarra Rossel, 2021; Ng et al., 2019; Tsakiridis et al., 2020; Zhong et al., 2021; Viscarra Rossel et al., 2022; Shen et al., 2022).

Just like the Gaussian pyramid, these powerful neural networks originate from image analysis. Similar to the Gaussian pyramid presented here, a CNN derives several resolutions and derivatives. The main difference is that these steps are part of the CNN itself, while a Gaussian pyramid is feature engineering in terms of pre-processing conducted before the application of a machine learning algorithm (Behrens et al., 2018a). The increase in prediction accuracy in soil spectroscopic studies when using CNNs compared to other modeling approaches is not very pronounced (Tsakiridis et al., 2020). This might reflect the finding of this study that cross-resolution interactions are negligible. Therefore, a comparison of the Gaussian pyramid approach with CNNs will be useful to further analyse the effects of multi-resolution interactions and derivatives.

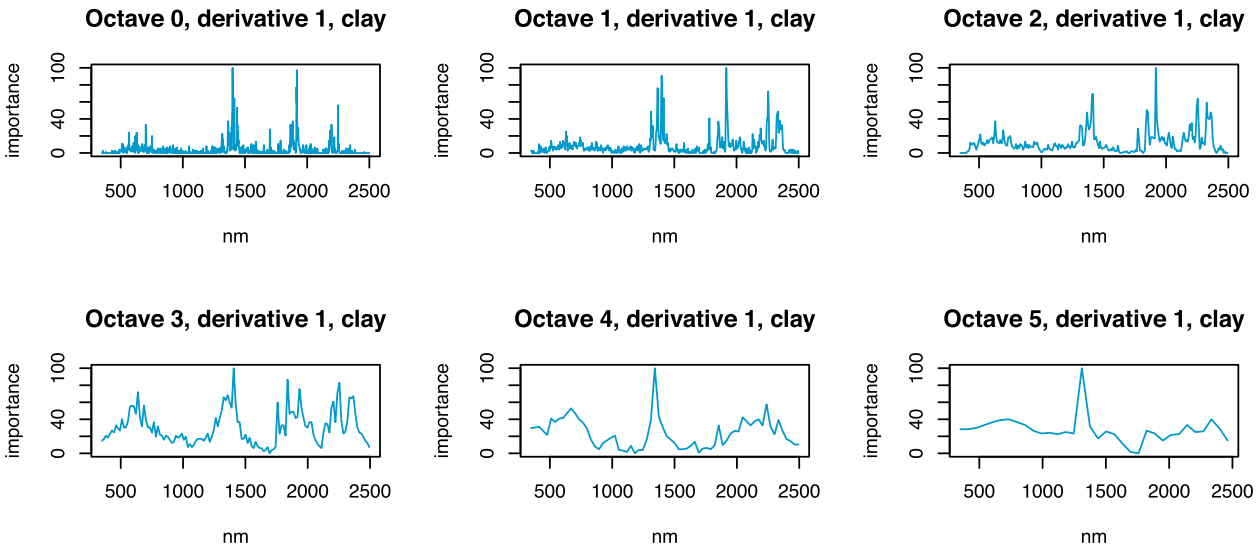

Fig. 5. Changes in feature importance values across different octaves of the 1st order derivative of the Gaussian pyramid for clay of the Australian dataset.

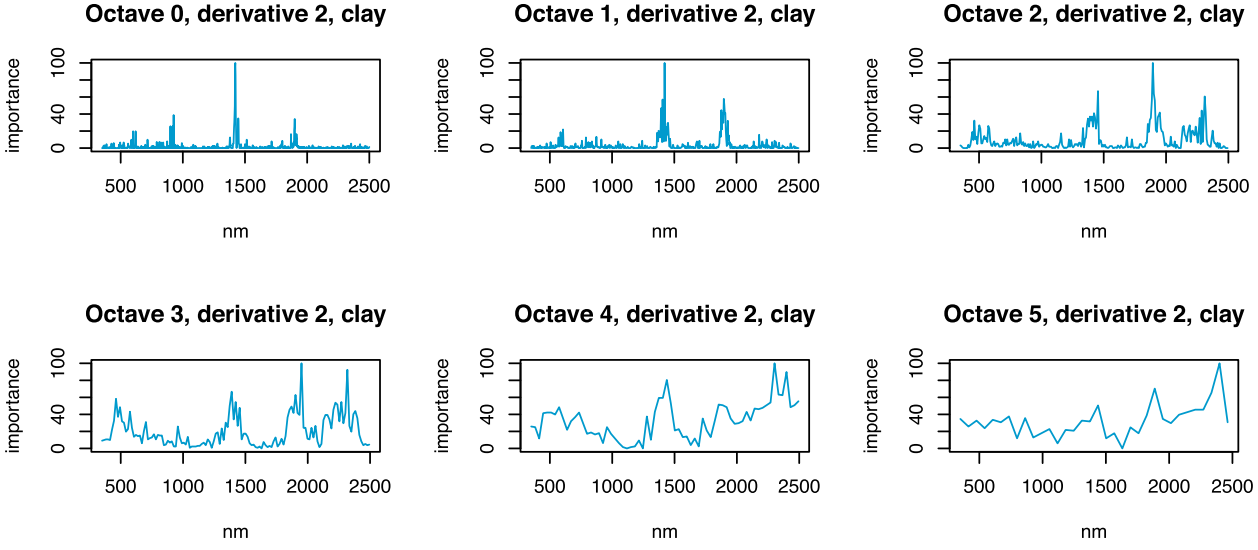

Fig. 6. Changes in feature importance values across different octaves of the 2nd order derivative of the Gaussian pyramid for clay of the Australian dataset.

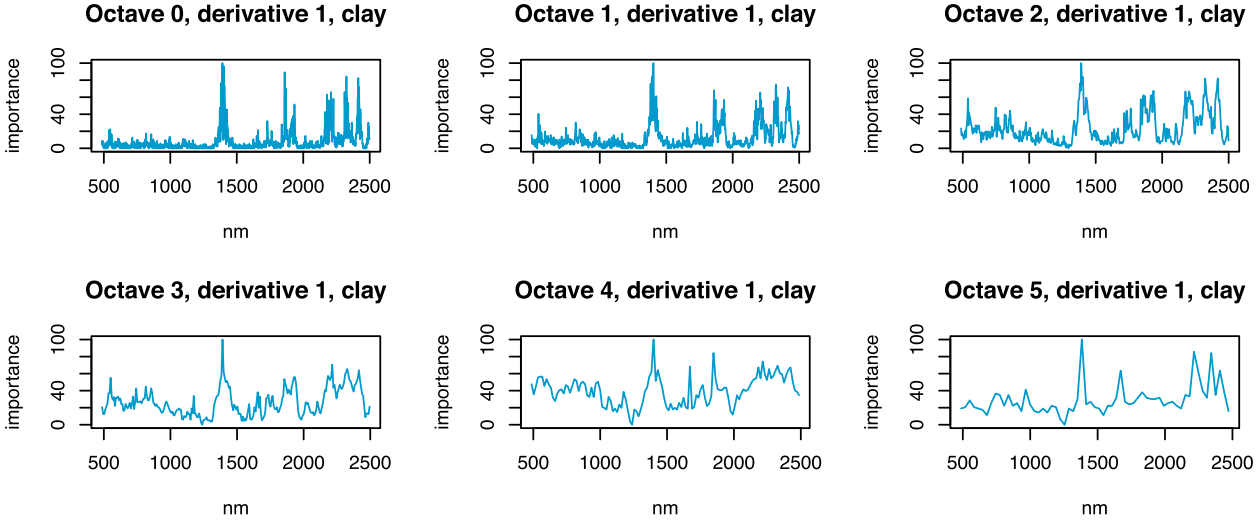

Fig. 7. Changes in feature importance values across different resolutions of the 1st order derivative of the Gaussian pyramid for clay of the LUCAS-DE dataset.

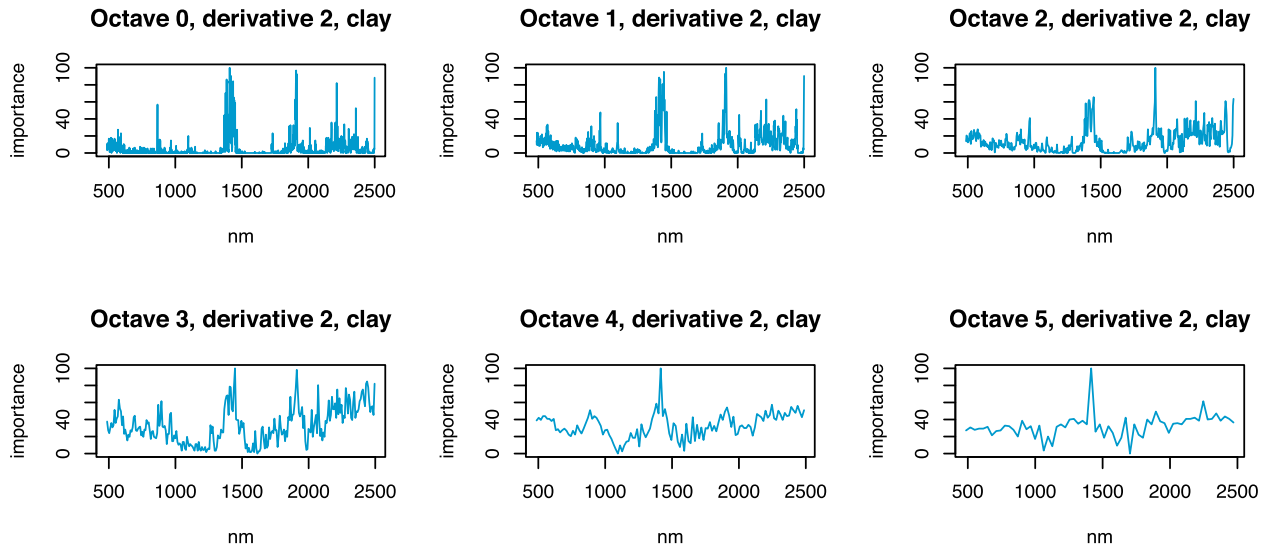

Fig. 8. Changes in feature importance values across different resolutions of the 2nd order derivative of the Gaussian pyramid for clay of the LUCAS-DE dataset.

5. Conclusions

The Gaussian pyramid provides a systematic solution for the analysis of spectra, to achieve accurate and interpretable predictions. Thus it can support knowledge discovery and decision making.

There were no prevalent context-dependent interactions or cross-resolution effects in the vis–NIR data sets tested. However, studies should be performed with mid infrared (MIR) spectra where we might expect more contextual interactions.

The advantage of single resolution models is their interpretability. We could show that the feature importance for a soil property becomes stable at the single resolution with the highest prediction accuracy even across different data sets. This underlines the importance of a careful selection of suitable resolutions for noise reduction, modeling and interpretation. A further advantage of the Gaussian pyramid is dimensionality reduction, which can allow to run context-dependent and automated model tuning for spectroscopic estimation in more rapid and memory-efficient ways. In this respect, the Gaussian pyramid offers an effective approach to modeling and analysing vis–NIR spectra.

Data and code availability

The LUCAS data are available online at https://esdac.jrc.ec.europa.eu/content/lucas-2009-topsoil-data after request. The code is available from the corresponding author upon reasonable request.

Declaration of Competing Interest

The authors declare that they have no known competing financial interests or personal relationships that could have appeared to influence the work reported in this paper.

Data availability

Data will be made available on request.

References

Adelson, E., Anderson, C., Bergen, J., Burt, P., Ogden, J., 1983. Pyramid methods in image processing. RCA Eng. 29.

Barnes, R.J., Dhanoa, M.S., Lister, S.J., 1989. Standard Normal Variate Transformation and De-Trending of Near-Infrared Diffuse Reflectance Spectra. Appl. Spectrosc. 43 (5), 772–777.

Behrens, T., Schmidt, K., MacMillan, R.A., Viscarra Rossel, R.A., 2018a. Multi-scale digital soil mapping with deep learning. Sci. Rep. 8 (1), 15244.

Behrens, T., Schmidt, K., MacMillan, R.A., Viscarra Rossel, R.A., 2018b. Multiscale contextual spatial modelling with the gaussian scale space. Geoderma 310, 128–137.

Behrens, T., Viscarra Rossel, R.A., Kerry, R., MacMillan, R., Schmidt, K., Lee, J., Scholten, T., Zhu, A.-X., 2019. The relevant range of scales for multi-scale contextual spatial modelling. Sci. Rep. 9 (14800).

Blanco, M., Coello, J., Iturriaga, H., Maspoch, S., Pezuela, C.D.L., 1997. Effect of Data Preprocessing Methods in Near-Infrared Diffuse Reflectance Spectroscopy for the Determination of the Active Compound in a Pharmaceutical Preparation. Appl. Spectrosc. 51 (2), 240–246.

Bruce, L., Li, J., 2001. Wavelets for computationally efficient hyperspectral derivative analysis. IEEE Trans. Geosci. Remote Sens. 39 (7), 1540–1546.

Burt, P., Adelson, E., 1983. The laplacian pyramid as a compact image code. IEEE Trans. Commun. COM 31, 532–540.

Delwiche, S.R., Reeves, J.B., 2004. The Effect of Spectral Pre-Treatments on the Partial Least Squares Modelling of Agricultural Products. J. Near Infrared Spectrosc. 12 (3), 177–182.

Gautam, R., Vanga, S., Ariese, F., Umapathy, S., 2015. Review of multidimensional data processing approaches for Raman and infrared spectroscopy. EPJ Techniq. Instrum. 2 (1), 8.

Ge, Y., Morgan, C.L.S., Thomasson, J.A., Waiser, T., 2007. A New Perspective to Near-Infrared Reflectance Spectroscopy: A Wavelet Approach. Trans. ASABE 50 (1), 303–311.

Getreuer, P., 2013. A Survey of Gaussian Convolution Algorithms. Image Processing On Line 3, 286–310. https://doi.org/10.5201/ipol.2013.87.

Guerrero-Colon, J.A., Mancera, L., Portilla, J., 2008. Image restoration using space-variant gaussian scale mixtures in overcomplete pyramids. IEEE Trans. Image Process. 17 (1), 27–41.

Igne, B., Reeves, J.B., McCarty, G., Hively, W.D., Lund, E., Hurburgh, C.R., 2010. Evaluation of Spectral Pretreatments, Partial Least Squares, Least Squares Support Vector Machines and Locally Weighted Regression for Quantitative Spectroscopic Analysis of Soils. J. Near Infrared Spectrosc. 18 (3), 167–176.

Jacques, L., Duval, L., Chaux, C., Peyré, G., 2011. A panorama on multiscale geometric representations, intertwining spatial, directional and frequency selectivity. CoRR abs/1101.5320. http://arxiv.org/abs/1101.5320.

Jones, A., Fernandez, U.O., Scarpa, S., 2020. Lucas 2015 topsoil survey. Publications Office of the European Union (KJ-NA-30332-EN-N).

Kuhn, M., Quinlan, R., 2020. Cubist: Rule- And Instance-Based Regression Modeling. R package version (2), 3 url:https://CRAN.R-project.org/package=Cubist.

Lindeberg, T., 2015. Image matching using generalized scale-space interest points. Journal of Mathematical Imaging and Vision 52 (1), 3-36, qC 20141218.http://urn.kb.se/resolve?urn=urn:nbn:se:kth:diva-153640.

Liu, L., Ji, M., Buchroithner, M., 2018. Transfer learning for soil spectroscopy based on convolutional neural networks and its application in soil clay content mapping using hyperspectral imagery. Sensors 18 (9) url: https://www.mdpi.com/1424-8220/18/9/3169.

Lowe, D.G., 1999. Object recognition from local scale-invariant features. In: Proceedings of the International Conference on Computer Vision-Volume 2, ICCV '99. IEEE Computer Society, USA, p. 1150.

McCarty, G.W., Reeves, J.B., Reeves, V.B., Follett, R.F., Kimble, J.M., 2002. Mid-Infrared and Near-Infrared Diffuse Reflectance Spectroscopy for Soil Carbon Measurement. Soil Sci. Soc. Am. J. 66 (2), 640–646.

Murdoch, W.J., Singh, C., Kumbier, K., Abbasi-Asl, R., Yu, B., 2019. Definitions, methods, and applications in interpretable machine learning. Proc. Nat. Acad. Sci. 116 (44), 22071–22080.

Ng, W., Minasny, B., Montazerolghaem, M., Padarian, J., Ferguson, R., Bailey, S., Mcbratney, A., 2019. Convolutional neural network for simultaneous prediction of

several soil properties using visible/near-infrared, mid-infrared, and their combined spectra. Geoderma.
Padarian, J., Minasny, B., McBratney, A., 2019. Using deep learning to predict soil properties from regional spectral data. Geoderma Regional 16, e00198 url: http://www.sciencedirect.com/science/article/pii/S2352009418302785.
Quinlan, J., 1993. Combining Instance-Based and Model-Based Learning. In: Machine Learning Proceedings 1993. Elsevier, pp. 236–243.
Rinnan, Å., van den Berg, F., Engelsen, S.B., 2009. Review of the most common pre-processing techniques for near-infrared spectra. TrAC Trends Anal. Chem. 28 (10), 1201–1222.
Savitzky, A., Golay, M.J.E., 1964. Smoothing and differentiation of data by simplified least squares procedures. Anal. Chem. 36 (8), 1627–1639.
Shao, X., Ma, C., 2003. A general approach to derivative calculation using wavelet transform. Chemometrics and Intelligent Laboratory Systems 69 (1), 157–165.
Shen, Z., Ramirez-Lopez, L., Behrens, T., Cui, L., Zhang, M., Walden, L., Wetterlind, J., Shi, Z., Sudduth, K.A., Baumann, P., Song, Y., Catambay, K., Viscarra Rossel, R.A., 2022. Deep transfer learning of global spectra for local soil carbon monitoring. ISPRS J. Photogrammetry Remote Sens. 188, 190–200.
Shen, Z., Viscarra Rossel, R.A., 2021. Automated spectroscopic modelling with optimised convolutional neural networks. Sci. Rep. 11 (1), 208.
Smith, L.N., 2018. A disciplined approach to neural network hyper-parameters: Part 1 - learning rate, batch size, momentum, and weight decay. CoRR abs/1803.09820. http://arxiv.org/abs/1803.09820.
Song, Y., Shen, Z., Wu, P., Viscarra Rossel, R.A., 2021. Wavelet geographically weighted regression for spectroscopic modelling of soil properties. Sci. Rep. 11 (1), 17503 url: https://www.nature.com/articles/s41598-021-96772-z.
Sonka, M., Hlavac, V., Boyle, R., 2014. Image Processing: Analysis and Machine Vision, 2nd Edition. CL-Engineering.
Stenberg, B., Viscarra Rossel, R., Mouazen, A., Wetterlind, J., 2010. Visible and Near Infrared Spectroscopy in Soil Science. Adv. Agronomy 107, 163–215.
Stevens, A., Nocita, M., Tóth, G., Montanarella, L., van Wesemael, B., 2013. Prediction of Soil Organic Carbon at the European Scale by Visible and Near InfraRed Reflectance Spectroscopy. PLoS ONE 8 (6), e66409.
Tóth, G., Jones, A., Montanarella, L., 2013. The LUCAS topsoil database and derived information on the regional variability of cropland topsoil properties in the European Union. Environ. Monit. Assess. 185 (9), 7409–7425.
Tsakiridis, N.L., Keramaris, K.D., Theocharis, J.B., Zalidis, G.C., 2020. Simultaneous prediction of soil properties from vnir-swir spectra using a localized multi-channel 1-d convolutional neural network. Geoderma 367, 114208.
Viscarra Rossel, R.A., Lark, R., 2009. Improved analysis and modelling of soil diffuse reflectance spectra using wavelets. Eur. J. Soil Sci. 60 (3).
Viscarra Rossel, R.A., Behrens, T., 2010. Using data mining to model and interpret soil diffuse reflectance spectra. Geoderma 158 (1–2), 46–54.
Viscarra Rossel, R.A., Behrens, T., Ben-Dor, E., Chabrillat, S., Demattê, J.A.M., Ge, Y., Gomez, C., Guerrero, C., Peng, Y., Ramirez-Lopez, L., Shi, Z., Stenberg, B., Webster, R., Winowiecki, L., Shen, Z., 2022. Diffuse reflectance spectroscopy for estimating soil properties: A technology for the 21st century. Eur. J. Soil Sci. 73 (4), e13271.
Viscarra Rossel, R.A., Walvoort, D., McBratney, A., Janik, L., Skjemstad, J., 2006. Visible, near infrared, mid infrared or combined diffuse reflectance spectroscopy for simultaneous assessment of various soil properties. Geoderma 131 (1–2), 59–75.
Viscarra Rossel, R.A., Behrens, T., Ben-Dor, E., Brown, D.J., Demattê, J.A.M., Shepherd, K.D., Ji, W., 2016. A global spectral library to characterize the world's soil. Earth Sci. Rev. 155.
Vohland, M., Ludwig, M., Harbich, M., Emmerling, C., Thiele-Bruhn, S., 2016. Using variable selection and wavelets to exploit the full potential of visible-near infrared spectra for predicting soil properties. J. Near Infrared Spectrosc. 24 (3), 255–269.
Wold, S., Sjöström, M., Eriksson, L., 2001. Pls-regression: a basic tool of chemometrics. Chemometrics and Intelligent Laboratory Systems 58 (2), 109–130, pLS Methods. http://www.sciencedirect.com/science/article/pii/S0169743901001551.
Yang, H., Kuang, B., Mouazen, A.M., 2012. Quantitative analysis of soil nitrogen and carbon at a farm scale using visible and near infrared spectroscopy coupled with wavelength reduction. Eur. J. Soil Sci. 63 (3), 410–420.
Zhong, L., Guo, X., Xu, Z., Ding, M., 2021. Soil properties: Their prediction and feature extraction from the lucas spectral library using deep convolutional neural networks. Geoderma 402, 115366 url: https://www.sciencedirect.com/science/article/pii/S0016706121004468.